THE JOURNAL OF PHYSICAL CHEMISTRY B

Article

pubs.acs.org/JPCB

The Entropic Cost of Polymer Confinement

Mark R. Smyda and Stephen C. Harvey*

School of Biology and Parker H. Petit Institute for Bioengineering and Bioscience, Georgia Institute of Technology, Atlanta Georgia 30332, United States

Supporting Information

ABSTRACT: The confinement of a polymer into a small space is thermodynamically unfavorable because of the reduction in the number of conformational states. The entropic penalty affects a variety of biological processes, and it plays an important role in polymer transport properties and in microfluidic devices. We determine the entropic penalty for the confinement of elastic polymer of persistence length P in the long-chain limit. We examine three geometries: (1) parallel planes separated by a distance d (a slit); (2) a circular tube of diameter d; and (3) a sphere of diameter d. We first consider infinitely thin (ideal) chains. As d/P drops from 100 to 0.01, $T\Delta S$ rises from $\sim 5 \times 10^{-4} kT$ to $\sim 30kT$ per persistence length for cases (1) and (2), with the entropic penalty for case (2) being consistently about twice that for case (1). $T\Delta S$ is $\sim 5kT$ per persistence length for confinement to a sphere when $d = P$, about twice the value predicted by mean field theory. For all three geometries, in the limit $d/P \gg 1$, the asymptotic behavior of ΔS vs d is consistent with the d^{-2} behavior predicted by theory. In the limit $d/P \ll 1$, the scaling of ΔS for slits and tubes is also consistent with earlier predictions ($d^{-2/3}$). Finally, we treat volume exclusion effects, examining chains of diameter $D > 0$. Confinement to a narrow slit or tube ($d/P \ll 1$) has the same entropic penalty as that for an ideal chain in a slit or tube with $d' = d - D$; in the weak confinement regime ($d/P \gg 1$), the entropic penalties are significantly larger than those for infinitely thin chains. When a chain of finite diameter is forced into a sphere or other closed cavity, the entropic confinement penalty rises without limit because there are no configurations available to the chain once its volume exceeds that of the cavity.

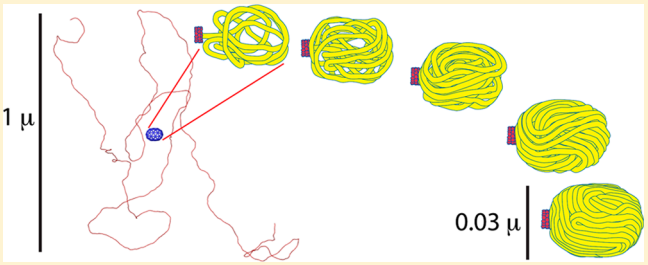

INTRODUCTION

The conformational entropy of a chain polymer makes a significant contribution to a wide range of physical properties, including elasticity, mobility in confined spaces, and miscibility with other polymers.[1−3] The entropic penalty associated with polymer confinement has important implications for the movement of polymers through gels,[4] polymer mixing,[5] the design of microfluidic devices for polymer fractionation,[6,7] and for biological processes such as the transport of proteins and nucleic acids through trans-membrane pores and pili,[8] and the packaging of genomes into RNA viruses[9] and DNA viruses.[10−14] Discussions of polymer entropy were pioneered by Paul Flory more than 60 years ago,[1] but several aspects of the problem of determining entropic confinement penalties remain unsolved.

There are three geometries to be considered: parallel planes separated by a distance d (a slit); a cylinder (tube) of diameter d; and a sphere of diameter d. We call these "1D", "2D", and "3D" confinement because the chain loses conformational freedom in one, two, and three dimensions, respectively. For each of these, there are two extreme cases, characterized by the ratio of the cavity size to the chain's persistence length, d/P. Strong confinement corresponds to the limit $d/P \ll 1$, while $d/P \gg 1$ is the regime of weak confinement. Between these extremes, there is a crossover region where $d \approx P$. We consider both infinitely thin chains (ideal chains) and chains with finite diameters, for which self-crossings are forbidden.

There have been several previous attempts to estimate the confinement penalties for ideal chains in cavities of various sizes and shapes. Casassa[15] estimated the partition coefficient, K, for very long Gaussian chains confined to spaces with d on the order of the radius of gyration, R_G. He treated the 1D, 2D, and 3D cases, finding in all of them that K is a sum of exponentials, with a factor of R_G^2/d^2 in every exponent. He noted that all three series converge very rapidly, so that each of the sums is well approximated by the first term. The free energy penalty is entirely entropic, and R_G^2 is proportional to the length of the chain, so Casassa is generally credited with being the first to suggest that, in the weakly confined limit ($d \gg P$), the penalty per unit length varies as d^{-2}. Other authors have presented alternative ways of reaching the same conclusion.[2,16] At the other extreme, in the strongly confined limit ($d \ll P$), both theory[17−21] and simulation[22] suggest that the cost is proportional to $d^{-2/3}$ for confinement of ideal chains to a tube. Odijk has argued that this result is easily generalized to the case of parallel planes.[20] In all the foregoing cases, there are modest differences in the estimates of the pre-exponential terms; we

Received: March 23, 2012
Revised: August 10, 2012
Published: August 20, 2012

resolve that issue in this article. Morrison and Thirumalai treated confinement to a sphere using a mean-field approach,[23] finding that, for small values of d/P, the entropic penalty in the 3D case is different for the 1D and 2D cases. Finally, Chen and Sullivan[24] estimated the penalties for ideal chains in slits in the range $0.1 \leq d/P \leq 10$, covering the crossover region where $d \approx P$.

The situation is more complex for chains of finite diameter because of excluded volume effects. For slits and tubes, DeGennes[16] argued that, in the weak confinement region, the penalty should scale as $d^{-1.7}$. For spherical confinement, the entropic penalty is not a linear function of chain length.[2,25] (It must grow monotonically, tending to infinity when the sphere is full since there are no conformations available for chains whose volumes exceed that of the sphere.) The length-dependence of the penalty can be determined numerically, using a molecular mechanics approach.[10−13] Alternatively, thermodynamic integration can be used to estimate the penalty,[26] with results supporting the predictions of blob theory[2] for packing densities in the range 1−10%. (The method can be extended up to packing densities of about 30%; those authors suggested a transition to a different power law behavior in this regime, apparently not recognizing that the free energy cost of confinement cannot be an extensive property of chain length for spherical confinement.) Scaling laws have been determined for the end-to-end distance of chains confined to slits and cylinders,[27,28] although those papers do not predict entopic costs.

Here, we provide a comprehensive solution to the problem, determining the entropic penalty per unit length for chains confined to a regular cavity of any size. We use a Monte Carlo approach to treat both ideal chains and chains with nonzero diameter. Our analysis ranges from very tightly confined chains ($d = 0.01P$) to very weakly confined chains ($d = 50P$ for finite chain diameter; $d = 100P$ for ideal chains). We treat all cases with a single approach, using no assumptions that cannot be tested. For chains with finite diameter, we introduce an algorithm that scales linearly with chain length to eliminate self-intersecting chains from consideration, allowing us to include volume exclusion effects in the determination of the 1D and 2D confinement penalties for very large values of d/P. (3D confinement of chains with volume exclusion requires separate methods, as discussed above.)

METHODS

Theoretical Framework. We seek to determine the entropic penalty when a semiflexible polymer chain of contour length L and persistence length P is confined to a small space (the constraining volume). Without loss of generality, we can place the constraining volume symmetrically around the origin of coordinates. We deal first with ideal chains, that is, chains with zero diameter. We will deal with the issue of volume exclusion below.

Consider the full thermodynamic ensemble of infinitely thin chains of fixed length L, i.e., a Boltzmann-weighted collection of all possible conformations in unbounded space. We divide this ensemble into two subensembles, one containing all chains that can be placed into the constraining volume without deformation (the constrained ensemble), and the other containing all chains that do not satisfy the constraint (the ensemble of violators). If the fraction of chains that comprise the constrained ensemble is f, then the entropic cost of confinement is

$$\Delta S = k \ln(f) \tag{1}$$

where k is Boltzmann's constant.

ΔS might be determined, at least in principle, by using a computer program to generate a large collection of chains of length L to approximate the full thermodynamic ensemble and then determining what fraction of these satisfy the constraint. Unfortunately, when d is on the order of P and the chain is very long, f will be so small that this approach becomes computationally intractable. Fortunately, as will be seen presently, we do not actually need the value of $f(L)$ to calculate $\Delta S(L)$ in the long-chain limit, which we define as $L \gg \max(d,P)$.

The determination of ΔS rests on two testable hypotheses.

Hypothesis 1: In the long-chain limit, the entropy of confinement is an extensive property, i.e., proportional to L:

$$\Delta S = k(C_0 - \alpha L) \tag{2}$$

For a given confinement geometry characterized by a single fixed distance d, α is a positive constant that depends only on d and P. Combining eqs 1 and 2, writing $C_0 = \ln(C')$ and solving for f gives

$$f(L) = C' e^{-\alpha L} \tag{3}$$

We know of no way to determine $f(L)$ for very long chains, but there is a quantity that we can determine, and whose exponential decay in the long-chain limit has the same decay constant, α. We define the fraction of chains in the ensemble of violators as

$$g(L) = 1 - f(L)$$

Consider a single chain, generated by growth from its left end. It satisfies the constraint until it reaches some length L_1 at which point it violates the constraint. A second chain, with a different configuration, will first violate the constraint at $L = L_2$. We define the function $h(L)$, the probability per unit length that a chain first violates the constraint when its length is between L and $L + dL$. Since an infinitely long chain must eventually violate the constraint,

$$\int_0^\infty h(l)\mathrm{d}l = 1.$$

Furthermore, $g(L)$ is a cumulative probability distribution,

$$g(L) = \int_0^L h(l)\mathrm{d}l$$

from which

$$h(L) = \frac{\mathrm{d}g(L)}{\mathrm{d}L} = -\frac{\mathrm{d}f(L)}{\mathrm{d}L}$$

In the long-chain limit, by eq 3,

$$h(L) = Ce^{-\alpha L} \tag{4}$$

where $C = \alpha C'$.

Equation 4 provides the possibility of determining α, and therefore ΔS, using a computational approach. We generate a collection of chains and estimate $h(L)$ by building a histogram, $N(L)$, of the distribution of lengths at which the first violation of the constraint occurs. If hypothesis 1 is true, then, in the long-chain limit, $N(L)$ will decay exponentially, and a plot of $\ln(N(L))$ vs L will be linear with slope $-\alpha$, for L greater than

some value, L_{crit}. By eq 2, the entropic penalty per unit length is αk, in the long-chain limit.

It is not evident how $N(L)$ will be affected by our choice of initial position and direction for generating the chains. Consider an initially oriented thermodynamic ensemble of chains of length L, obtained by bringing the left end of every chain in the full ensemble to a common point (the origin, for example) and rotating all chains so that all the initial tangent vectors point in the same direction (along the x-axis, say). The initially oriented ensemble is identical to the full thermodynamic ensemble in that it contains all possible chain conformations, not just those that satisfy the distance constraint. Since we have changed the orientations of the chains, the functions $f(L)$, $g(L)$, and $h(L)$ will be different than for the original ensemble, particularly for values of L on the order of d. In the long-chain limit, however, the behavior of the right end of the growing chain should become independent of the position and orientation of the chain's left end. This leads us to believe that the decays of $f(L)$ and $h(L)$ will still be asymptotically exponential, and that the decay constant will be identical to that of the original ensemble. We state that this as a testable three-part hypothesis.

Hypothesis 2: For any initially oriented thermodynamic ensemble, eq 4 remains valid in the long-chain limit. The pre-exponential factor C does depend on the position and orientation of the left end of the chains, but α does not. The decay constant α depends only on d and P.

To test hypotheses 1 and 2 and to determine entropic penalties, we generate chains starting with various initial positions and orientations, and we measure the asymptotic slope of plots of $\ln(N(L))$ vs L. We model polymer chains using wormlike chain (WLC) models.[29] The fine-grained (FG) WLC model has 147 elements per persistence length, while the coarse-grained (CG) WLC model has 25. These models mimic DNA (P = 50 nm; rise per residue = 0.34 nm), with one base pair per element in the FG model and about six base pairs per element in the CG model. For ideal chains, the diameter of each element is zero. We also investigate excluded volume effects, using models where each element consists of a bead having a diameter of 3 nm, again mimicking DNA. With excluded volume, a chain is eliminated from the thermodynamic ensemble if it collides with itself before hitting the wall of the confining volume. Under conditions of weak confinement of ideal chains, we also carry out simulations using the freely jointed chain (FJC) model. (See Supporting Information for detailed methods.)

This approach bears a superficial resemblance to the configurational bias Monte Carlo (CBMC) method.[22] Both start with initially oriented chains. CBMC uses a biasing potential to enhance sampling, which requires a subsequent renormalization step to correct for the bias. Our approach uses no biases, eliminating potential errors associated with post hoc corrections.

As described in detail below, ideal chains are modeled by a series of bonds of length b, connected by joints that allow isotropic bending. The FJC has no energy penalty for bending. In the WLC model, bending is opposed by an angular energy term, parametrized so that the model has the correct persistence length, P. Parameters are chosen to simulate the DNA double helix (P = 50 nm).

Wormlike Chain Model. In the WLC model, the angle between successive bonds is defined by the dot product of unit vectors along successive bonds

$$\cos\theta = \frac{\vec{b}_i \bullet \vec{b}_{i+1}}{|\vec{b}_i||\vec{b}_{i+1}|}$$

The deformation energy for bond angle bending has the standard harmonic form,[30] $E(\theta) = (a/2)(\theta - \theta_0)^2$, where a is the force constant, and θ_0 is the equilibrium angle (zero for the WLC). This produces a bend angle probability distribution function[31]

$$P(\theta) = A \sin\theta \, e^{-a\theta^2/2kT}$$

where A is a normalization factor, and the factor $\sin\theta$ arises from integration over the surface of the sphere defined by $0 \le \theta \le \pi$. The force constant is chosen by requiring the mean value of $\cos\theta$ to satisfy Schellman's equation for the persistence length[29]

$$P = \frac{b}{1 - \langle\cos\theta\rangle}$$

At T = 300K, a persistence length of 50 nm requires that $a = 6.096 \times 10^{-12}$ erg (87.833 kcal/mol) for the fine-grained FG model (b = 0.34 nm). For the coarse-grained CG model (b = 2.0 nm), $a = 1.013 \times 10^{-12}$ erg (14.597 kcal/mol).

We independently verified the persistence lengths of both the FG and CG models by generating large ensembles of chains of different lengths and determining the slopes in plots of the mean-square end-to-end distance vs L. In the long-chain limit, the slopes were both $2P$, within statistical error, as required.[2,3]

Freely Jointed Chain Model. The x, y, and z components of each new bond are chosen randomly from uniform probability distributions, $-1 \le b_i \le 1$ (i = x,y,z), guaranteeing a spherically uniform distribution of bond directions. The bond length is then normalized to $b = 2P$ (the Kuhn length), as required by the FJC model. Finally, the new bond is translated to extend the chain from the end of the previous bond.

We examined some cases for the ideal chain using two or three different models (FG WLC, CG WLC, and FJC). In all such cases, models with fewer internal degrees of freedom slightly overestimate the penalty (Table 1), presumably because they underestimate the proportion of very compact conformations.

Excluded Volume Effects. To investigate the effects of finite chain diameter, we used WLC chains with bead diameter $D = 0.06P$ (D = 3 nm, the approximate diameter of the hydrated DNA double helix under physiological conditions, i.e., pH 7; 150 mM ionic strength). Using a conventional algorithm, the search for self-intersection in a chain containing N beads would require the examination of $\sim N^2/2$ interactions; this would be computationally prohibitive for examining confinement in very large volumes, where N can be on the order of 10^6 or more before the chain collides with the wall. We reduced the computational burden by partitioning space into a virtual grid of small cubes (voxels), each of which is identified by a triplet of indices, (i,j,k). The i,j,k mapping of coordinates to voxels is explicitly defined in a hash table only when a bead's center of mass resides within. As terminal bead N is generated, the voxel corresponding to the location of that bead is populated. Testing for self-intersection is performed via hash lookup of grid cells within the range $i - 1$, $i + 1$; $j - 1$, $j + 1$; $k - 1$, $k + 1$, and the distance from bead N to each of the previous beads in this space is computed and compared to diameter D. If self-intersection is found, the chain is discarded, and generation of a new chain is begun. Because beads are volume excluded, there

Table 1. Entropic Penalty Per Persistence Length (in units of kT) for Confinement of Ideal Chains[a]

d/P	parallel planes separated by distance d		circular tube of diameter d		sphere of diameter d	
0.01	23.5		50		n.d.	
0.02	14.6		31		n.d.	
0.05	7.8		17		n.d.	
0.1	4.7		10		n.d.	
0.2	2.9		6.4		n.d.	
0.5	1.4		3.2		14.5	
1	0.71	*0.81*	1.78	*2.02*	5.0	
	0.72 (cg)		1.82 (cg)		5.1 (cg)	
2	0.30	*0.39*	0.79	*1.2*	1.7 (cg)	
	0.32 (cg)		0.79 (cg)			
5	0.074	*0.090*	0.20 (cg)	*0.21*	0.36 (cg)	*0.37*
	0.082 (cg)					
10	0.024 (cg)	*0.027*	0.058 (cg)	*0.063*	0.103 (cg)	*0.109*
20	7×10^{-3}		*0.017*		*0.029*	
50	1.2×10^{-3}		2.8×10^{-3}		4.9×10^{-3}	
100	3×10^{-4}		7×10^{-4}		1.2×10^{-3}	

[a]Italic font indicates calculations using the FJC model. Normal font indicates calculations using the WLC models; for these, the fine grain (FG) model was used except for those cases indicated by (cg), where the coarse grain (CG) model was used; n.d. = not determined.

exists an upper bound on voxel capacity, thus making the algorithm $O(N)$ linear in both time and memory requirements. We ensure completeness by setting the length of the edge of each voxel to D, so no collision is possible outside of the nearest 27 cells.

Data Analysis. Values of α were determined by weighted linear regression of $\ln(N)$ vs L/P using *R* (R Foundation for Statistical Computing, Vienna, Austria; http://www.R-project.org). The lower limit of L/P for each analysis (L_{crit}) was chosen by visual inspection of the semilog plots, with analysis confined to regions of clearly linear decay. After each analysis, the regression line was plotted over the full range of original data, to verify the quality of the fit, and to be certain that only the region of linear decay had been used (Figures 1−3 and S1−S9, Supporting Information). Values of L_{crit} for all of the cases studied are given in Table S1, Supporting Information. We estimate that values of ΔS are accurate to within 2−5% for the 1D and 2D cases and for large spheres ($d/P \geq 5$) and that the errors in ΔS are on the order of 5−10% for smaller spheres. For example, the average value of the entropic penalty for confinement of an ideal chain to a sphere with $d/P = 1$ is $5.0kT$ for the fine-grain model (Table 1). The most extreme excursion from this value is about 8%, occurring when chain generation begins very close to and parallel to the wall of the sphere (Figure S3b, Supporting Information).

RESULTS AND DISCUSSION

Ideal Chains. For all cases, 1D, 2D, and 3D confinements and all values of d/P, terminal decays for $h(L)$ are single exponentials for ideal chains, confirming hypothesis 1 (Figures 1−3 and S1−S7, Supporting Information). The initial decay of $h(L)$ does depend on the position and orientation of the left end of the chain, and initial decays can be quite complex (Figures 2−3 and S3, Supporting Information). However, all decay curves are asymptotically single-exponential; for a given geometry and fixed d, all have the same limiting decay constant within statistical error, confirming hypothesis 2.

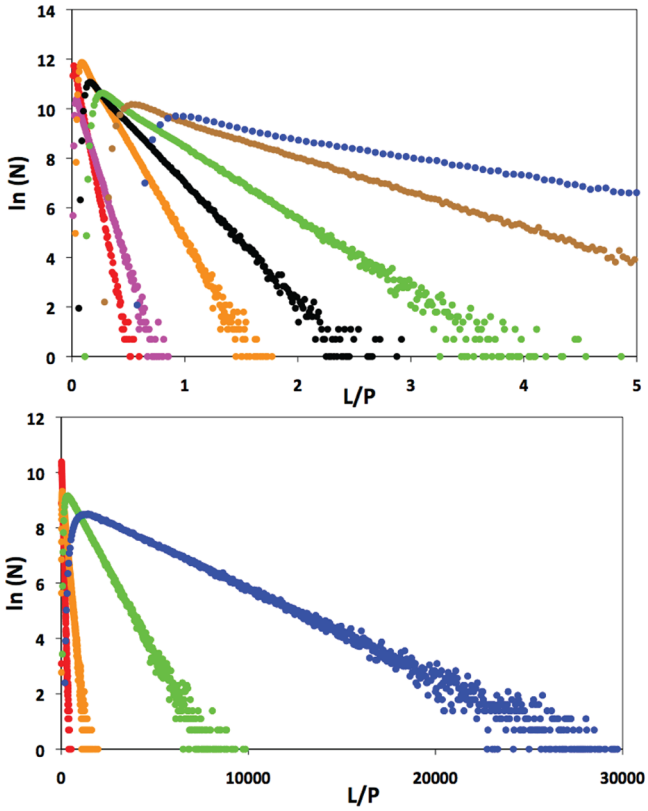

Figure 1. Probability distribution functions for first violation of the constraint, $N(L)$, for ideal chains in a slit of width d, when chain generation begins midway between and parallel to the confining planes. Upper panel: d/P = 0.01 (red), 0.02 (magenta), 0.05 (orange), 0.1 (black), 0.2 (green), 0.5 (brown), and 1 (blue). Lower panel: d/P = 10 (red), 20 (orange), 50 (green), and 100 (blue). Note the very different length scales in the two panels.

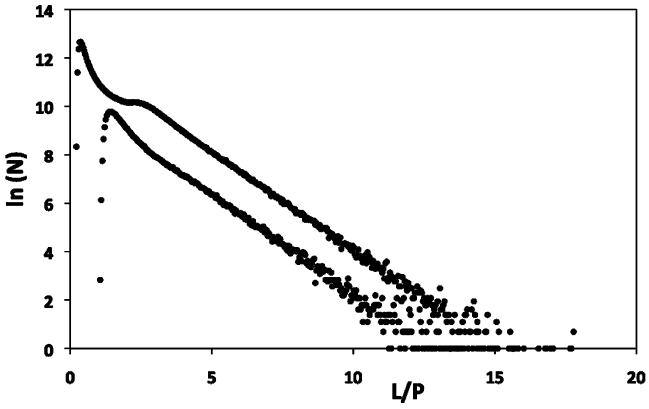

Figure 2. Dependence of the decay of the probability distribution function $N(L)$ on the position of the start of chain generation, for ideal chains in a circular tube of radius $r = d/2 = P$, centered on the x-axis. The lower curve shows an ensemble of 5×10^5 chains whose left ends all lie at the origin, while the upper curve is an ensemble of 5×10^6 chains whose left ends all lie at $x_0 = z_0 = 0$ and $y_0 = 0.8r$. In both cases, initial chain generation is in the $+x$ direction. The asymptotic decays have the same slope.

Figure 4 summarizes the entropic penalties for all cases that we have studied; Table 1 provides more detail for ideal chains. The penalty is on the order of kT per persistence length when $d/P \approx 1$. Examination of Figure 4 shows that, in both the limit $d \ll P$ and in the limit $d \gg P$, $\log(T\Delta S)$ is a linear function of

dx.doi.org/10.1021/jp302807r | J. Phys. Chem. B 2012, 116, 10928−10934

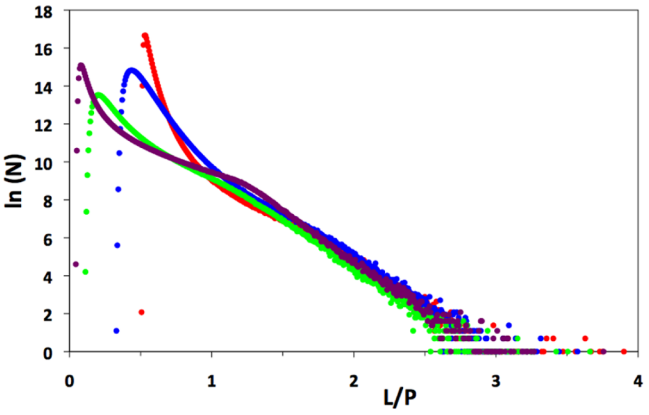

Figure 3. $N(L)$ for confinement of an ideal chain to a sphere of diameter $d = P$. The left ends of all chains lie on the y-axis ($x_0 = z_0 = 0$), and all initial tangent vectors point in the $+x$ direction. The y-coordinate of the starting point of chain generation is expressed as a fraction of the radius $r = d/2$: $y_0 = 0$ (red); $0.4r$ (blue); $0.8r$ (green); and $0.96r$ (purple). In the long-chain limit, the slopes of the decay curves are identical.

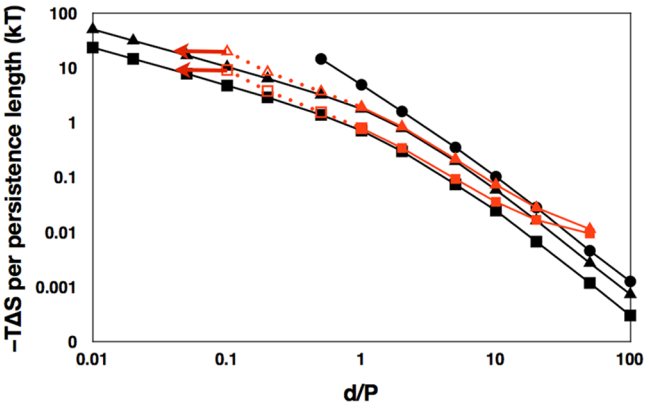

Figure 4. Confinement penalties for ideal chains ($D = 0$, black) and one chain of nonzero diameter ($D = 0.06P$; red), in the long-chain limit. Results are shown for confinement into slits (squares), circular tubes (triangles), and spheres (circles). The red curves are dashed for values of $d/P < 1$ because D becomes a significant fraction of d in this region. The red arrows show that, when $d = 0.1P$, the entropic penalty for a chain of nonzero diameter D is the same as it would be for an ideal chain of diameter $d' = d - D = 0.04P$. (There is no red curve for spherical confinement; when chains with nonzero diameter are confined to spheres, ΔS is not an extensive property of L.)

$\log(d/P)$ for ideal chains, i.e., ΔS is proportional to d^w, where w is the slope of the log−log plot.

For ideal chains in the limit $d \gg P$, the entropic penalties in all three cases, confinement into slits, tubes, and spheres, are asymptotic to the d^{-2} dependence first predicted by Casassa.[15] For $d/P = 100$, Casassa's estimates of ΔS are about 10% higher than our values for all three cases, so his estimates of limiting behavior were excellent.

In the limit $d/P \ll 1$, our results confirm predictions that the limiting entropies of infinitely thin chains scale as $d^{-2/3}$ for cylindrical confinement[17−22] and planar confinement.[20] The behavior of ΔS when $d < P$ appears to be different for spherical confinement than for slits and tubes (Figure 4), as previously predicted.[23] Clearly, confinement to small spheres is different from planar or cylindrical confinement because conformational space is unbounded in the 1D and 2D cases, but not in 3D confinement. Unfortunately, the decays of $h(L)$ are so rapid for diameters smaller than P that we cannot calculate the entropic penalties for small spheres ($d/P < 0.5$), so we cannot determine the scaling law in the limit $d/P \ll 1$.

In the crossover region where $d \approx P$, there are two previous studies that are relevant here. First, Morrison and Thirumalai[23] used a mean-field approach to estimate the confinement penalty for ideal chains confined to small spheres; their estimate is

$$\frac{\Delta F}{kT} \approx \frac{0.56LP}{R^2} - 1.1\frac{P}{R} + \frac{3}{2}\ln\left(\frac{LP}{R^2}\right) + 0.44$$

where $R = d/2$ is the radius of the sphere. (This is a corrected form of their eq 38, kindly provided by D. Thirumalai.) To compare this estimate with our result, consider a sphere of diameter $d = P$. The above expression then becomes

$$\frac{\Delta F}{kT} \approx \frac{2.24L}{P} - 2.2 + \frac{3}{2}\ln\left(\frac{L}{P}\right) + \frac{3}{2}\ln(4) + 0.44$$
$$= \frac{2.24L}{P} + \frac{3}{2}\ln\left(\frac{L}{P}\right) + 0.32$$

In the long-chain limit, the linear term dominates, and the estimated value of ΔF is $\sim 2.24kT$ per persistence length, about half our value of $5kT$. Second, Chen and Sullivan[24] determined the entropic penalties for confinement of ideal wormlike chains into slits over the range $0.1 \le d/P \le 10$ in the long-chain limit. Their values are typically about 10% higher than those reported here, so agreement between our two studies is excellent, in spite of very different approaches.

The analysis of eqs 1−4 is valid beyond a critical length, L_{crit}, for every case except spherical confinement of chains with finite diameter. L_{crit} does depend on d, and on the starting position and orientation of the chain. Approximate values of L_{crit} for infinitely thin chains, obtained by inspection of plots of $\ln(N)$ vs L (Figures 1−3 and S1−S7, Supporting Information), are tabulated in Table S1, Supporting Information; results for chains of finite diameter are not significantly different. L_{crit} is of the order of d for tight and modest confinement, and it rises to hundreds of persistence lengths for very weak confinement.

It should be noted that different models give slightly different estimates of the entropic penalties for ideal chains (Table 1). In those cases where we calculated ΔS with both WLC and FJC models, we find that, without exception, the WLC model gives slightly lower values than the FJC model. In addition, estimates for ΔS are consistently slightly lower for the fine-grained (FG) model than for the coarse-grained (CG) model. Taken together, these results suggest that models with fewer internal degrees of freedom systematically underestimate the proportion of very compact conformations. (As an extreme example, we note that each element of the FJC model is a rod of length $2P$. There are no configurations of the FJC chain inside a sphere of diameter $d < 2P$, so the FJC model would face an infinite entropic penalty to confinement inside such a sphere.

Excluded Volume Effects. With 1D and 2D confinement, hypotheses 1 and 2 and eq 4 remain valid for chains with finite diameter (Figures S8 and S9, Supporting Information). When such chains are confined to spheres (3D confinement), ΔS is not an extensive property of L: the entropic penalty rises monotonically without limit as the chain fills the sphere and reduces the remaining free volume. The penalties in spherical confinement of chains with finite diameter can be determined

dx.doi.org/10.1021/jp302807r | J. Phys. Chem. B 2012, 116, 10928−10934

using a molecular mechanics model, by integrating the force vs distance curve as the chain is pushed into the sphere.[10−13]

The effects of finite chain diameter are summarized in Table 2 and Figure 4. In the tight confinement regime ($d \ll P$), self-collisions are very rare; the entropy penalty for a chain of diameter D in a slit or tube of characteristic dimension d is the same as that for a chain of zero diameter in a slit or tube with characteristic dimension $d' = d - D$ (red arrows in Figure 4). Under conditions of moderate confinement ($d/P \approx 0.5-2$), excluded volume effects are minimal for both 1D and 2D confinement because self-collisions are much less frequent than collisions with the wall.

Table 2. Entropic Penalty Per Persistence Length (in units of kT) for Confinement of Chains with Diameter $D = 0.06P$

d/P	parallel planes separated by distance d	circular tube of diameter d
0.1	9.1	20
0.2	3.8	8.4
0.5	1.55	3.7
1	0.79	1.9
2	0.34	0.84
5	0.094	0.22
10	0.036	0.074
20	0.017	0.028
50	0.009	0.011

In the weak confinement regime ($d \gg P$), the entropic penalty is substantially larger for chains of finite diameter than for those of zero diameter (Figure 4). The explanation for this is quite simple. Consider the full thermodynamic ensemble of ideal chains of length L ($D = 0$). If each chain is now given a finite diameter, it either has no self-intersections (so it remains in the ensemble) or it passes through itself at one or more points, so it has a nonphysical structure and is eliminated from the ensemble. The probability of self-intersection is higher in more compact chains than in extended chains, so chains in the full thermodynamic ensemble are, on average, more extended than those in the full ensemble of zero diameter chains. (For example, the mean-square end-to-end distance is larger for chains with finite diameter than for infinitely thin chains: Figure S11, Supporting Information.) Since finite diameter makes chains more extended, it also increases the probability of collision with the walls of the confining volume, increasing the fraction of chains in the ensemble of violators. This increases the entropic penalty of confinement when $d \gg P$.

The arguments in the previous paragraph explain why the limiting behavior in the weak confinement regime does not follow the prediction made by DeGennes[16] that the penalty should scale as $d^{-1.7}$ for confinement of chains of nonzero diameter into slits and tubes. Instead of the predicted power law behavior, the curves of $T\Delta S$ vs d/P are nonlinear in the weak confinement region (Figure 4). The terminal slopes in Figure 4 in the limit of weak confinement are approximately −0.6 and −1.0 for the 1D and 2D cases, respectively, significantly smaller than the predicted slope of −1.7. The free energy penalties are therefore substantially larger than those predicted by DeGennes. We hypothesize that scaling theory[16] fails to accurately describe the configurational probability distributions for extremely long chains (L on the order of hundreds of persistence lengths), where configurations with one or more crossings must be detected and eliminated from the ensemble of unconfined chains. Similar considerations probably apply to blob theory.[2] Previous computer simulations that examined confinement of chains with finite diameter[26] used chains that are relatively short (up to 2048 monomers), and the radius of the confining spheres were expressed relative to the chain's radius of gyration; clearly this approach cannot be used to reach the long-chain limit examined here.

The cumulative probability of self-intersection rises monotonically with N, with the probability per unit length of self-intersection being essentially constant once L exceeds ∼$10P$ or so (Figure S10, Supporting Information). From the terminal slope of this plot, we see that, if a very long free chain is extended by one persistence length, it has a probability of 8.6×10^{-3} of colliding with itself. Following the argument presented immediately after eq 4, we might consider the conformational free energy penalty of chain extension to be $8.6 \times 10^{-3} kT$ per persistence length. This exceeds the confinement penalty for ideal chains in volumes with values of d/P on the order of 20−50 (Figure 4; Table 1), so self-collision dominates collisions with the wall for slits, tubes, and spheres that are larger than this. Again, this emphasizes that, in the very weak confinement regime, chains of finite diameter that do eventually collide with the walls come from an ensemble that is more extended than the corresponding ensemble of ideal chains.

CONCLUSIONS

Considerations of conformational entropy are relevant, and sometimes dominant, in the behavior of single polymers, polymer melts, and biological macromolecules. As one example, we have found that, when double-helical DNA is packaged into small viral capsids, the conformational entropy penalty is as large as the enthalpic penalty from electrostatic repulsions.[10,12] As another example, consider microfabricated entropy traps, which are more efficient than traditional gels for the isolation of large polymers.[6,7] These devices contain a rectangular channel with alternating wide (∼500−1000 nm) and narrow (∼50−100 nm) regions (slits). An electric field is used to drive DNA molecules ranging from 3 kbp to 150 kbp (20 to 1000 persistence lengths) into the narrow slit, which is only one or two persistence lengths wide. The associated entropic penalty, from Figure 4, is on the order of $0.5kT$ per persistence length, or $10-500kT$ for molecules in this size range.

The methods developed here allow the determination of the entropic confinement penalties for ideal chains (zero diameter) and chains that are prohibited from self-intersection (finite diameter), including 1D, 2D, and 3D confinement. As seen in Figure 4, our approach covers a range of 4 orders of magnitude, centered on the crossover region at $d = P$, where behavior shifts from tight confinement to weak confinement. We have confirmed the scaling laws proposed by others for ideal chains, allowing extrapolation of the results to all values of d/P, and we have successfully extended our approach to include chains with nonzero diameter, where self-intersection is not allowed. None of the methods reviewed in the introduction are capable of treating such a broad range of problems. Finally, we note that our methods can be easily extended to treat irregular geometries, branched polymers, and other systems.

ASSOCIATED CONTENT

Supporting Information

Eleven additional figures, showing the decay curves of $\ln(N)$ vs L/P for a variety of cases with ideal chains (Figures S1−S7) and chains with nonzero diameter (Figures S8−S9); a semilog plot of the probability distribution function for the first self-collision

of a chain with finite diameter (Figure S10); and a comparison of the mean-square end-to-end distance for a chain of nonzero diameter with that of an ideal chain, as a function of chain length (Figure S11). One additional table, giving approximate values of L_{crit}, the lower boundary of long-chain limit for all cases involving ideal chains. This material is available free of charge via the Internet at http://pubs.acs.org.

AUTHOR INFORMATION

Corresponding Author

*Tel: 404-444-3551. Fax: 404-894-0519. E-mail: steve.harvey@biology.gatech.edu.

Author Contributions

S.C.H. designed and implemented the algorithm for ideal wormlike chains and carried out the simulations on these. M.R.S. designed and implemented the algorithm for the FJC model and for chains of nonzero diameter, and he carried out the simulations on those, confirming, in the process, the results for ideal chains.

Notes

The authors declare no competing financial interest.

ACKNOWLEDGMENTS

Supported by NIH grant R01 GM70785 to S.C.H. This work is the result of spirited discussions with Rob Phillips and Bill Gelbart. We are grateful to Jeff Z. Y. Chen for providing the data from ref 24, allowing a direct comparison of our results with his.

REFERENCES

(1) Flory, P. J. *Principles of Polymer Chemistry*; Cornell University Press: Ithaca, NY, 1953.
(2) Grosberg, A. Y.; Khokhlov, A. R. *Statistical Physics of Macromolecules*; AIP Press: New York, 1994.
(3) Dill, K. A.; Bromberg, S. *Molecular Driving Forces*; Garland Science: New York, 2003.
(4) Smisek, D. L.; Hoagland, D. A. *Science* **1990**, *248*, 1221−3.
(5) Robertson, R. M.; Smith, D. E. *Proc. Natl. Acad. Sci. U.S.A.* **2007**, *104*, 4824−7.
(6) Han, J.; Craighead, H. G. *Science* **2000**, *288*, 1026−9.
(7) Fu, J.; Yoo, J.; Han, J. *Phys. Rev. Lett.* **2006**, *97*, 018103.
(8) Muthukumar, M. *Annu. Rev. Biophys. Biomol. Struct.* **2007**, *36*, 435−50.
(9) Yoffe, A. M.; Prinsen, P.; Gopal, A.; Knobler, C. M.; Gelbart, W. M.; Ben-Shaul, A. *Proc. Natl. Acad. Sci. U.S.A.* **2008**, *105*, 16153−8.
(10) Locker, C. R.; Fuller, S. D.; Harvey, S. C. *Biophys. J.* **2007**, *93*, 2861−2869.
(11) Petrov, A. S.; Boz, M. B.; Harvey, S. C. *J. Struct. Biol.* **2007**, *160*, 241−8.
(12) Petrov, A. S.; Harvey, S. C. *Structure* **2007**, *15*, 21−7.
(13) Harvey, S. C.; Petrov, A. S.; Devkota, B.; Boz, M. B. *Phys. Chem. Chem. Phys.* **2009**, *11*, 10553−10564.
(14) Harvey, S. C.; Petrov, A. S.; Devkota, B.; Boz, M. B. *Methods Enzymol.* **2011**, *487*, 513−543.
(15) Casassa, E. F. *J. Polym. Sci., Part B: Polym. Phys.* **1967**, *5*, 773−778.
(16) DeGennes, P.-G. *Scaling Concepts in Polymer Physics*; Cornell University Press: Ithaca, NY, 1979.
(17) Helfrich, W.; Harbich, W. *ChemScript* **1985**, *25*, 32−36.
(18) Khokhlov, A. R.; Semenov, A. N. *Phys. A* **1981**, *108*, 546−556.
(19) Khokhlov, A. R.; Semenov, A. N. *Phys. A* **1982**, *112*, 605−614.
(20) Odijk, T. *Macromolecules* **1983**, *16*, 1340−1344.
(21) Odijk, T. *Macromolecules* **1986**, *19*, 2313−2328.
(22) Dijkstra, M.; Frenkel, D.; Lekkerkerker, H. N. W. *Phys. A* **1993**, *193*, 374−393.
(23) Morrison, G.; Thirumalai, D. *Phys. Rev. E: Stat., Nonlinear, Soft Matter Phys.* **2009**, *79*, 011924.
(24) Chen, J. Z. Y.; Sullivan, D. E. *Macromolecules* **2006**, *39*, 7769−7773.
(25) Sakaue, T.; Raphaël, E. *Macromolecules* **2006**, *39*, 2621−2628.
(26) Cacciuto, A.; Luijten, E. *Nano Lett.* **2006**, *6* (5), 901−5.
(27) Cordeiro, C.; Molisana, M.; Thirumalai, D. *J. Phys. II* **1997**, *7*, 433−447.
(28) Morrison, G.; Thirumalai, D. *J. Chem. Phys.* **2005**, *122* (19), 194907.
(29) Schellman, J. A. *Biopolymers* **1974**, *13*, 217−226.
(30) McCammon, J. A.; Harvey, S. C. *Dynamics of Proteins and Nucleic Acids*; Cambridge University Press: London, U.K., 1987.
(31) Locker, C. R.; Harvey, S. C. *Multiscale Model. Simul.* **2006**, *5*, 1264−1279.